43rd AIAA/ASME/ASCE/AHS/ASC Structures, Structural Dynamics, and Materials Con
22-25 April 2002, Denver, Colorado

AIAA-2002-1337

A JOINED-WING STRUCTURAL WEIGHT MODELING STUDY

Maxwell Blair*
Robert A. Canfield**

Abstract

An integrated design process for generating high fidelity analytical weight estimations of joined-wing concepts is described. Elements of configuration, structures, aerodynamics and aeroelastic analyses are incorporated. Drag and loads are modeled for sizing fuel and structures to meet range and loiter requirements. The joined-wing is a radical departure from the world's inventory of vehicles. We are motivated because the joined-wing concept may offer weight savings where structural stiffness is a design constraint.

Two crucial non-linear phonomena contribute to structural failure: large deformation aerodynamics and geometric non-linear structures. A correct model of the non-linear aeroelastic model offers the possibility of a successful design that leverages these non-linear effects to the benefit of joined-wing designs.

The process reported here is useful because physics-based data is automatically fed into making high level decisions in the unprecedented design of a joined-wing concept. The authors hope this work will contribute toward future development of weight-competitive concepts for commercial and USAF use.

The current process required the integration of several software products, including the Adaptive Modeling Language (AML), MSC.ASTROS, MSC.NASTRAN and PanAir. Special functions were added into the AML environment, which automate the structure/aero interface and non-linear trim.

Background and Goals

The joined-wing concept has been studied by a number of designers and specialists since 1986 when Wolkovich [1] published his concept. Livne has provided a valuable survey paper on these technical developments [2]. Blair et. al. presented their work [3] with the development of a joined-wing design model with variable configuration integrated with automated aerodynamic and structures assessment in a single environment. The current paper is a direct follow-on to this referenced work.

Complementing the work presented here is the work of Weisshaar and Lee [4] who have provided significant insight into the important role of flutter in constraining joined-wing design. Another publication of interest is the blended-wing-body design study presented by Wakayama [5]. Here, a common environment has been developed for physics-based modeling of this innovative concept. Another unifying approach toward design is presented in [6]. Here, surface geometry is structured to serve as a unifying medium, with the benefit that this saves on data storage where a number of disciplines interact.

The weight advantages of joined-wing design are far from realized. Indeed, some advocates have concluded the joined-wing is not weight competitive with existing commercial carriers. However, these conclusions were based on relatively simple models without the benefit of non-linear aeroelastic modeling. With the development of nonlinear analysis and design tools, researchers at AFRL and AFIT are revisiting the joined-wing concept as a weight-competitive alternative.

The goal of the current effort is to combine configuration design with high fidelity FEM-based weight modeling in order to converge on a configuration which simultaneously satisfies the following:

- Range requirements (fuel scheduling)
- equilibrium in lift and pitching moment
- stress in static aeroelastic equilibrium.

The particular challenge for a joined-wing design is to overcome the nonlinear buckling response of the aft wing. The current work examines the buckling response of a linear fully stressed design (FSD), but

* Aerospace Engineer, Air Force Research Laboratory, Air Vehicles Directorate, Wright-Patterson AFB, Ohio, AIAA Associate Fellow
** Associate Professor, Air Force Institute of Technology, Department of Aeronautics and Astronautics, Wright-Patterson AFB, Ohio, AIAA Associate Fellow

the process is being established to iterate for the nonlinear case.

AML for System Design Integration

The Adaptive Modeling Language (AML) [7] has been aggressively marketed as an engineering design modeling environment for software developers. As such, it was clear to the authors that AML facilitated the joined-wing design process reported in this paper. AML features which facilitate the process are (a) strongly object-oriented programming language making full use of parent-child relationships and object inheritance (b) native-geometry objects based on Parasolids and Shapes geometry engines (c) interpreted code for run-time interaction and compiled-code for numerical speed (d) automated memory management and (e) automated dependency-tracking and demand-driven calculations.

The AML interface drives the analysis modules. PanAir is used as the aerodynamic surface paneling method to calculate steady air loads. ASTROS is used for FSD. MSC.Nastran is used for the buckling and the geometrically nonlinear analysis.

Basic AML Objects and Enhancements

The design of a joined-wing involves complex geometry beyond what is normally associated with a traditional wing. Here, the first author has taken the tools provided by TechnoSoft and, following standard object inheritance procedures, has tailored a set of objects to serve our needs. The process of developing the joined-wing object has paralleled the development of a set of basic AML objects. Some of the objects, which form the building blocks for the joined-wing object, were reported in [3]. Basic geometric objects were developed to form curves, extruded meshes and Hermite (cubic parametric) surface networks. At the geometric component design level were developed for airfoils, wing panels, extruded wings, wing-tips and joined-wings. These objects are fully controllable. For example, where wing thickness is an important conceptual design feature, a single parameter has been incorporated for its control. In addition, the airfoil object has been enhanced to include tabulated Reynolds-dependent drag polar data.

Figure 1. The airfoil object

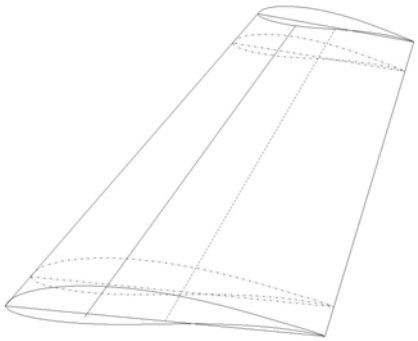

Figure 2. Wireframe geometry to control wing-panel

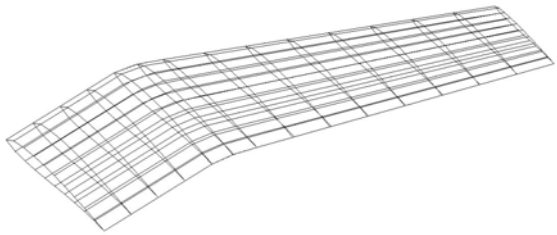

Figure 3. The wing object (web geometry)

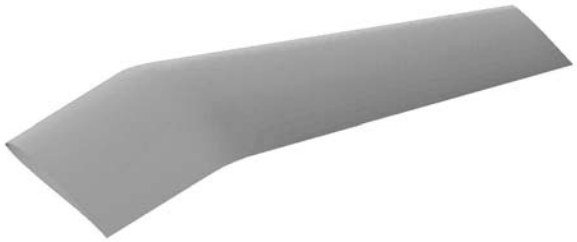

Figure 4. The wing object (surface geometry)

Joined-wing object: A collection of wing-panels, wing-tip, trajectories and contours were used to create a blended surface for the following applications: IGES and ParaSolid surface representations for CFD calculations, panel definitions to drive PanAir input and a structural finite element modeler to drive input for a structural optimization code ASTROS and NASTRAN. This object is controlled with the following properties: scaleable (thickness and chord) airfoils at key locations, twist at key locations, fore-aft wing separation in x and z, component sweep, taper and chord. The shape of the wing tip scales automatically or can be easily crafted to form a variety of shapes such a crescent wing. The web resolution is controlled for each analysis (and IGES model) separately.

Aerodynamic Modeling

PanAir: PanAir [8] provides the aerodynamic model for large deformations. The element partitioning is variable. The baseline analysis model is depicted in Figure 5. The number of panels is a model variable and is generally between 500 and 1000 depending on convergence. However, little was done to explore aerodynamic convergence with panel refinement. The overall load is calibrated to achieve a fixed lift and therefore, only the distribution of pressure is effected with panel refinement.

PanAir is a linear aerodynamic solver using the technique of boundary elements, otherwise referred to as a aerodynamic paneling method. Surface geometry is "body-fitted" with an array of quadrilateral panels. Continuous surface singularities (both sources and doublets) are distributed using a number of schemes to meet a number of needs.

In this work aerodynamic loads were generated from the predicted pressures in the true normal direction. Although the panels form a "sharp" leading edge and the pressure is assumed normal to the panel, we chose to ignore that information and use the true normal generated by the geometric surface object. The reason for this is to add some element of consistency between the CFD solvers and PanAir. We expect this geometric inconsistency will disappear with PanAir model refinement or its replacement by CFD.

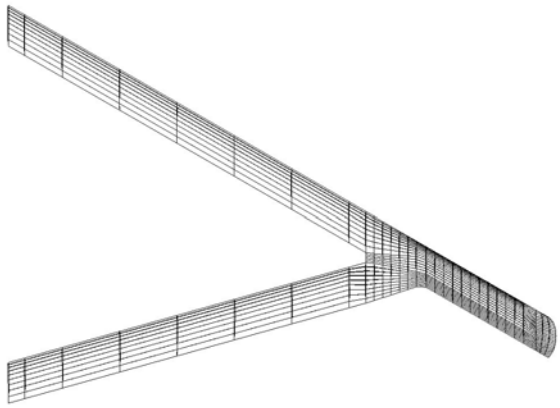

Figure 5. Web Geometry for Joined-wing Concept with 30 degrees tip sweep

The aerodynamic mesh incorporates high aspect ratio panels along the inboard portions of the wing and a portion of the outboard wing. The merged region and the wing tip have lower aspect ratio panels to capture spanwise variations in flow. Figure 5 shows that a structured mesh on a joined-wing requires doubling the chord-wise mesh on the outboard leg of the wing. However, this works to our advantage in accurately capturing the outboard portion as we study the loads in the wing joint region. The PanAir model incorporates 12 networks with associated abutments. Each network is a matrix of panels with rows and columns. For instance, the top surface of the aft wing has 8 rows and 7 columns of panels to form a single PanAir network.

Flat trailing wakes were placed behind the most aft edge. The wake attached to the trailing edge along the forward and inboard portion of the wing is pre-shaped. No further effort was expended to study the influence of wake shape.

Integrated Pressures. PanAir integrates values for rigid-body forces (lift, drag, sideslip) and moments (pitch, roll, yaw). We assume these integrated values are based on constant pressure distributions on each panel and the bordering doublets. PanAir also prints out a file (AGPS) with interpolated pressures at element corner points. For redistributed loads on the structural model, we chose to approximate a smooth pressure distribution based on the pressures at the element corners. However, it turns out there can be a discrepancy of up to 5% between the PanAir integration (based on constant distribution) and our integrated values (based on the interpolated pressure) for a given angle of attack. However, this will not hinder the design of a structure where the total lift is

specified and distribution of pressure is subsequently calculated.

Trim and Stability Considerations [9]: The center of pressure, defined as $x_0 = x_{cp} = -M_{LE}/C_L$, is used to determine the point of static equilibrium. M_{LE} is usually a negative value, so the center of pressure is usually a positive value.

Vehicle trim is controlled with angle-of-attack α and aft-wing-root-twist δ. The trim condition is determined with a series of linear Taylor series approximations.

$$[1] \quad \begin{Bmatrix} C_L - C_{L0} \\ C_M - C_{M0} \end{Bmatrix} = \begin{bmatrix} \left(\frac{dC_L}{d\alpha}\right) & \left(\frac{dC_L}{d\delta}\right) \\ \left(\frac{dC_M}{d\alpha}\right) & \left(\frac{dC_M}{d\delta}\right) \end{bmatrix} \begin{Bmatrix} \alpha - \alpha_1 \\ \delta - \delta_0 \end{Bmatrix}$$

C_{L0} and C_{M0} are the Taylor reference point in lift and moment coefficient. Two values of δ (δ_0, δ_1) and three values of α (α_0, α_1, α_2) are selected. Panair is very efficient at running multiple angles-of-attack and not efficient with calculations associated with non-linear geometric changes generated by wing-twist. The Taylor reference points (C_{L0} and C_{M0}) are associated with α_1 and δ_0. The target values of C_L and C_M are N_zW /qS and 0 respectively. N_z is the load-factor. W is the weight. The zero moment is calculated at the center of mass. The system of two equations is solved iteratively for α and δ. Panair is run again for this trim condition and the pressures are again distributed as loads in the structural design.

The aerodynamic center is located at $x_{ac}/c = -C_{M\alpha}/C_{L\alpha}$. The position of the aerodynamic center with respect to the center of mass determines the dynamic pitch stability for the vehicle. Again, $dC_M/d\alpha$ is usually a negative value so the aerodynamic center is usually a positive value.

It turns out that the joined wing concept requires special attention in pitch balance to avoid adverse trim with negative lift on the aft wing resulting in excess drag. This drives the requirement to maintain outboard wing sweep as an important design variable. The zero sweep case is depicted in Figure 6 in order to emphasize this point.

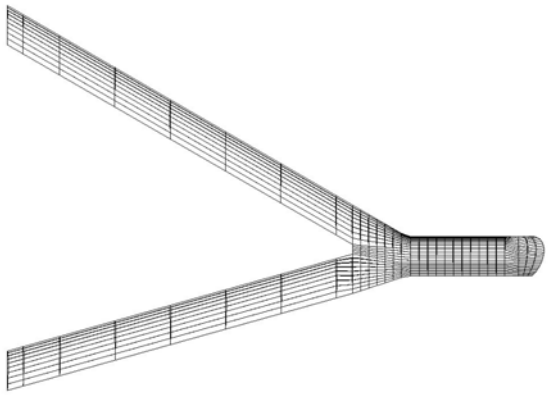

Figure 6. Web Geometry for Joined-wing Concept with 0 degrees tip sweep

Drag Build-Up: Aircraft designers decompose drag contributions into three components: (1) parasite drag (2) induced drag (3) compressibility drag. A special utility was developed using incompressible experimental data [10] to account for parasite drag, and ignores compressibility drag. Once high-Reynolds number data is obtained, the procedure will calculate a sectional lift coefficient along each chord-wise column of panels. Values of compressible drag coefficient will then be interpolated from the tabulated two-dimensional drag data. In this way, drag is summed over the wing. While this approach is not reliable for accurate prediction of absolute drag (including fuselage and propeller drag, etc.), it is useful in comparing design variants.

Structural Modeling

The structural meshes for the upper and lower skins are identical. In addition, the substructure is idealized as a complete "egg-crate" connecting each top membrane element with its lower counterpart. Soft substructure elements were added at the wingtip leading and trailing edge to facilitate the load transfer between the aerodynamic and structural models. While the incorporation of "soft" leading and trailing edge structure is non-conventional modeling practice, its inclusion helps us to understand natural load paths for conceptualizing the substructure design.

Structural Solution Procedure: The solution procedure for converging on geometric non-linear equilibrium involves use of the standard NASTRAN [11] procedure to solve the global buckling equations. The linear stresses due to flexible, trimmed air loads were used to determine a FSD in ASTROS [12], which was checked for buckling in NASTRAN.

Finally, gradient-based optimization in NASTRAN will be used to satisfy the buckling constraint.

Aero-Structures Interaction

Non-linear analysis requires geometrically large deformations to be addressed. A specialized interface between aerodynamics and structures was generated in AML.

The structures-to-aero process finds the intersection between normal vectors at control points in the (undeformed) PanAir model and planar elements in the (undeformed) structural FEM model. The structural deformation between surface grid points is simply interpolated assuming a flat surface.

The aero-to-structures process is a bit more involved. Each aerodynamic panel is subdivided and the pressure over each panel is interpolated based on pressure values output at each corner of the PanAir model. The center, normal and integrated-force for each sub-panel is computed and the intersecting structural element is identified. The force is then applied to each element and subsequently to each corner grid point. The force is partitioned according to the proximity to each corner grid, thus maintaining equivalent energy in going from the aerodynamic distribution of pressure to the equivalent structural load at the grid points.

The solution procedure for converging on non-linear equilibrium involves a series of corrections starting with a rigid model with rigid loads and ending with flexible loads on a deformed structure.

The Joined-Wing Design Process

The concept design process is a matter of balancing all design considerations until requirements have been met and the system optimized for cost or performance. A successful design requires a number of conflicting design decisions to be resolved. At the top level, we have to ask if the joined-wing vehicle design has the required range and loiter capability. This question can be answered if we know all the weights and aerodynamic drag for all segments of the mission profile. At the detailed structural level, we have to ask if the vehicle is sufficiently stiff (aeroelasticity) and strong to carry all anticipated loads. These two design activities are mutually dependent.

Designing for Fuel: To start the process, we seek the fuel required for a specified mission. We could use sophisticated flight path integration schemes (*cf.* Ref. 2); however, the Breguet range equation provides important insight in the fundamental design of this joined-wing concept, where V is velocity, C is specific fuel consumption, L/D is the lift to drag ratio and W is weight. The range equation is inverted in order to solve for the fuel requirement for a fixed mission range.

$$[2] \quad R = \left(\frac{V}{C}\right)\left(\frac{L}{D}\right)\ln\left(\frac{W_{i-1}}{W_i}\right)$$

Aerodynamic efficiency is realized with high L/D. While lift (L) is a direct consequence of weight (structures, payload, etc), aerodynamics takes primary responsibility for drag (D). Elements that contribute to drag are viscosity and induced losses. These relate primarily to geometric "wetted area" and "aspect ratio" respectively.

Designing for Trim and Stability: For vertical equilibrium in level flight, lift must equal the weight. For a high altitude concept, this may require significant velocity to generate adequate dynamic pressure to remain aloft in thin air. This may become a limiting factor. At the same time, the long endurance mission requires a significant amount of fuel at takeoff. This has to be considered in modeling the takeoff condition.

At the same time, the design has to consider pitch equilibrium. An efficient wing design requires that all lifting surface components contribute positive lift. For the joined-wing depicted in Figure 5, the center of mass must be located sufficiently aft to maintain both pitch equilibrium global positive lift. The concern is that with the center of mass moved too far aft, the system may become unstable in pitch with the center of mass aft of the aerodynamic center. It may be corrected with an active control system (for negative static stability) or the outboard wing component may be designed with less aft sweep.

System Analysis Elements: The following outline lists the parallel system analysis elements involved in converging on a design solution. Each element starts with an "intelligent" assumption to be revisited later. For instance L/D is influenced by vehicle weight and trim. However, one starts with the initial guess.

1. Mission
    - 1.1. Lift/Drag (L/D)
        - 1.1.1. Shape
            - 1.1.1.1. Rigid
            - 1.1.1.2. Flexible
        - 1.1.2. Mach
        - 1.1.3. Reynolds Number
    - 1.2. Component Weights
        - 1.2.1. Empty Weight
            - 1.2.1.1. Structure
            - 1.2.1.2. Non-Structural

1.2.2. Fuel Weight
1.2.2.1. Breguet range equation
2. Vehicle Trim
2.1. Equilibrium
2.1.1. Lift
2.1.2. Pitch
2.2. Stability
3. Shape Definition
3.1. Configuration
3.2. Rigid
3.3. Flexible
4. Loads
4.1. Aerodynamic
4.1.1. Shape
4.1.1.1. Rigid
4.1.1.2. Flexible
4.1.1.3. Trimmed
4.1.2. Aero Mesh
4.1.3. Pressure Calculations
4.1.3.1. Conversion to Loads
5. Structures
5.1. FEM Mesh
5.2. Loads Formulation
5.3. Stress
5.3.1. Geometric-Non-linear
5.4. Buckling
5.5. Structural Weight

Recursive Dependencies: As indicated, the steps outlined above require initial assumptions at each stage to be repeatedly corrected until convergence has been achieved.

Non-linear aeroelastic analysis is a recursive process involving aerodynamic and structural analyses which share a common deforming surface. Starting with a rigid outer surface definition, the recursion is roughly as follows:

- Update aero mesh with deformed structure
- Calculate pressure distribution
- Integrate pressure into forces at FEM grid points
- Calculate structural deformation

The deformed shape influences the drag and therefore the fuel requirement is altered.

- Integrate pressure into lift
- Obtain drag from tabulated data
- Calculate fuel requirement
- Redistribute fuel
- Revisit trim analysis
- Generate structural loads
- Revisit non-linear aeroelastic analysis

The deformed shape and new structural weights influences the trim condition

- Compensate by moving component masses
- Calculate stability derivatives
- Solve system for new trim condition
- Recalculate new pressure distribution
- Revisit non-linear aeroelastic analysis

New structural design using fully-stressed optimization influences vehicle weight which forces everything to be reconsidered. The stress optimization procedure involves a combination of procedures for calculating minimum weights:

- Fully stressed optimization
- Buckling optimization

System Design Convergence Procedure: A number of unknowns went into the sizing of the joined-wing concept. The two primary drivers are minimum fuel weight and minimum structural weight. Each of these unknowns is calculated in the following iterative fashion. The constraints in this process are:

1. Required mission (range)
1.1. ingress, loiter, egress
2. Load requirements for structural design
2.1. Pull-up @ 2.5-g's (due to gust)

There is no one unique path in converging on an acceptable design. Our accomplishment to date is really in the development of this process by which we can design a joined-wing concept in the presence of mutual dependencies with physics-based models. At this point, we focus on what we have accomplished in developing a viable joined-wing design.

The Joined-Wing Design

The Design Mission: This study uses the Global Hawk mission profile. Global Hawk data approved for public release (unlimited distribution) 12 August 1999.

1) Takeoff zero ft altitude at 0 NM range
2) Climb to 50K ft altitude for 200 NM
3) Cruise at 50K ft for 3000 NM ingress
4) Loiter at 50-65K ft altitude for 24 hours
5) Cruise at 50K ft altitude for 3000 NM egress
6) Descend to zero ft altitude for 200 NM
7) Land at zero ft altitude

Here, we assume an L/D of 24 is achievable at Mach 0.6 for ingress and egress. PanAir will be used to calculate L/D for the flexible wing from full to empty fuel conditions to update the Breguet equation. Between 11 and 20 kilometers altitude, the standard speed of sound is 295 m/s. The velocity on ingress and egress is 178 m/s. Assume velocity at loiter is 118 m/s. Assume coefficient of brake horsepower, $C_{bhp,}$ is 0.55 and propeller efficiency is assumed to be 0.8.

	ingress	loiter	egress
Range	3000 nm 5,550 km	NA	3000 nm 5,550 km
Duration	NA	24 hr 8.64E4 sec	NA
Velocity	0.6 Mach @50K ft 177 m/s	0.4 Mach to 65K ft 118 m/s	0.6 Mach @50K ft 177 m/s
C (SFC)	2.02E-4 (1/sec)	1.34E-04 (1/sec)	2.02E-4 (1/sec)
Dynamic pressure	2939 Pa	638 Pa	2939 Pa
Wa/Wb	1.32	1.62	1.33

Table 1. Baseline Aerodynamic Parameters

The Baseline Configuration

Configuration: The configuration is driven by a significant number of parameters, some of which are listed in Table 1. A schematic is provided in Figure 6 to help interpret these parameters. For this study, this list of parameters is more extensive than the two authors can address for the initial conceptual design. Hence, these parameters are grouped and prioritized according to importance to aerodynamic and structural efficiency for this study. They are also prioritized as they relate to rigid 6dof stability and configuration in order to point out the extent of work for true design integration.

This high-risk design concept will not jeopardize the conclusions reached in this study. Twist actuation could be accomplished by conventional control surfaces.

S_{ib}	26.00 m
S_{ob}	6.25 m
c_{rf}	2.50 m
c_{ra}	2.50 m
c_m	2.50 m
c_t	2.50 m
x_{fa}	22.00 m
z_{fa}	7.00 m
Λ_{ib}	30 deg
Λ_{ob}	30 deg
Airfoil	FX-60-126-1
Calculated Planform Area	145.0 m^2
Calculated Wing Volume	52.2 m^3

Table 2. Baseline Configuration Parameters

Wing Thickness: Wing thickness is influenced by availability of Conformal Load-bearing Antenna Structures (CLAS) technology. Without CLAS, wing thickness is constrained to contain a large antenna array panel facing the nominal horizon. This results in a thick and less efficient wing. CLAS wraps around the wing and potentially results in a thin wing. Increasing wing thickness enables more fuel to be stored in the wings. From a structures perspective, increased wing thickness results in a more stiff and thus lighter wing. Increased flexibility results in larger deformations and more aeroelastic interaction. The skins have lower aspect ratio elements than the aerodynamic panel model in order to govern the resulting substructure element aspect ratio, which can have a large effect on the wing stiffness.

Aft Wing Vertical Offset: A larger vertical offset results in a joined-wing concept with more bending stiffness. The normal vector of the nominal "plane" contains the joined-wing points in the direction of least stiffness. With no vertical offset, the normal is also vertical and the wing is most flexible in the normal direction. With increasing (aft wing) vertical offset, this normal vector begins to point forward away from the lift vector and toward the drag vector, which is much smaller. Thus, the wing deforms less for the same lift. The load path starts at the wing tip and naturally heads in a direction to achieve a state of least global strain energy. Consider a simple pull-up maneuver with the load vector pointing up. Along the aft wing compression and bending loads are present and pass into the vertical tail and the fuselage. Along the front wing, there are tension and bending loads that pass into the fuselage. The two paths meet and equilibrate in the fuselage.

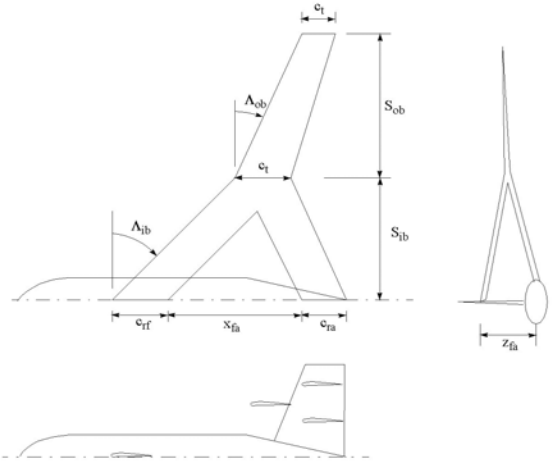

Figure 6. Planform Configuration

Twist-Actuated Aft Wing: Pitch control is effected with twist actuation of the aft wing. The aft wing pivots about a shaft at the wing root. Actuation is realized with pushrods extending up the vertical tail.

The aft wing provides ample control power with minimum drag. Aft-wing stiffness is an important feature in the successful design of this novel control effector concept. Torsional stiffness must be low and bending stiffness must be high. Compliant structural design may help realize this concept. Spanwise slits in the aft wing skin will soften the aft wing in torsion. Reinforcement with soft sub-structure will allow large deformations without excessive torsional control power.

Materials: The material for the wing structure is currently isotropic aluminum, although composite materials are anticipated for sensor-craft. Sensor-pointing requirements are expected to make wing structural design to be stiffness driven. To account for fatigue life constraints material allowables were reduced to 103 *MPa* in normal stress and 55 *MPa* for shear. A minimum structural thickness of 0.125 *cm* was imposed.

Baseline Empty Weights: The mass model is comprised of structural weight, payload, engine, fuel and other systems. The assumed gross take-off weight and the fuel weights (mass) are recorded in the Table 3. Fuel is carried in the wing and fuselage. Fuel distribution is controlled at the top level. This vehicle model assumes all fuel evenly-distributed through the wing and none in the fuselage for maximum load alleviation. Based on Global Hawk (Wto = 25,600 lb), we assume take-off gross weight for this larger joined-wing concept to be 28,600 kg (63,000 lb). Take the product of all the weight fractions (1.3*1.6*1.3) times the take-off gross weight to obtain the calculated landing weight of 10,050 kg. Thus, the mission consumes 18,600 kg of fuel.

	Mass (kg)	Weight (lbs)
Payload	2220	4880
Engine	450	1,000
Fuel	18,580	40,870
Wing Structure	6,070 (guess)	13,350 (guess)
Fuselage Structure	1200	2640
Tail Structure	100	220
TOTAL	28,620 (assumed)	62,960 (assumed)

Table 3. Baseline Weights

The engine weight is based on Torenbeek's [13] formula, where [$0.35 < W_E < 0.55$] lb/hp. For target L/D of 24 and lift of 30,800 lbs, drag is 1,280 lb. At a velocity of 584 f/s we get a power requirement of P = (1280 * 584) = 7.48E5 ft-lb/s = 1353 hp. With Torenbeek's formula, this results in an engine weight, W_E = (1353 * 0.45) = 609 lbs (not installed). Raymer [14] approximates the installed engine weight is $W_{E\text{-installed}} = 2.575W_E^{0.922} = 2.575*609^{0.922}$ = 951 lbs. This weight is approximated as 1000 lbs in the table.

The payload weight of nearly 5,000 lbs accounts for electronic gear. The wing structural weight is guessed at 13,000 lb. The non-structural weights are to be appropriately distributed in the design model at various points in the trajectory (different fuel) and subsequently reflected in the aeroelastic FEM model. The fuselage weight is taken from a formula in [15] for commercial vehicles. We arrive at an estimation of 2640 lb for the fuselage weight.

A convergence procedure is proposed here to close on the fuel weight and structural weight to meet load requirements, including fuel and inertial relief, recursively based on structural weight.

Structural weight is comprised of wing-skin, wing substructure, tail (parametric) and overall fuselage (parametric model). The sub-structures for this model are "fully-populated". This egg-crate substructure does not represent actual production substructure. However, if the minimum gauge is not constrained and allowed to approach small values during fully stressed design process, then one expects the resulting weight will be representative of production substructure (minus fasteners etc). Of course, this does not take local buckling and cutouts into consideration. These details are normally approximated at the conceptual stage and accurately accounted only in the detailed design.

Keep in mind that these figures are all based on a number of assumptions that must be explored in the design process outlined here. Indeed, the claim of this paper is that no one really knows how much this joined-wing concept will weigh until a high fidelity study is completed.

Fuel Weight: The baseline wing has the volume 52.2 m^3 to carry 42,300 *kg* of fuel (kerosene density of 810 kg/m^3). The range analysis, Eq.(2), calls for 18,580 *kg* of fuel, which occupies 44% of the available volume for fuel in the wing. For structural analysis, fuel stored in the wing provides "inertial" relief, which counters the aerodynamic load. Therefore, more fuel results in less structural load for this design model.

Aerodynamic Trim: In order to generate reasonable static aerodynamic loads, a trim analysis was performed to realize static equilibrium for the rigid airplane using the weights calculated up to this point.

Parasite drag was assumed constant, C_D=0.01, while induced drag was calculated by PanAir. After two iterations, we converged on the following conditions:

	Ingress	Loiter
C_L	0.981	1.15
C_D	0.0403	0.054
L / D	24.3	21.3
Aero center	14.5 *m*	14.6 *m*
Center of Pressure	13.3 *m*	14.2 *m*

Table 4. Rigid Trimmed Loads

Results

The integrated rigid pressure on the top skin (Fig. 7) illustrates the significance of leading edge suction as generated by our PanAir model. This is partially offset by the leading edge drag on the lower. These pressures are independently interpolated for the upper and lower networks. One inconsistency is the pressures on the top network and the bottom network do not agree at the leading edge.

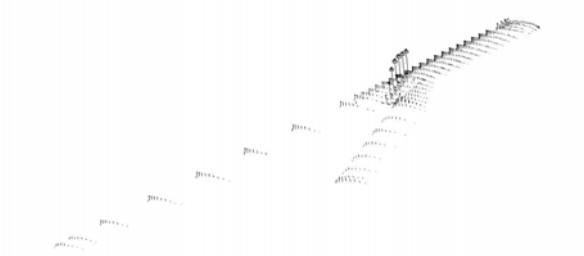

Figure 7. Rigid Trimmed PanAir Pressure Vectors on the Top Skin

Figure 8 depicts the forces as they have been transferred from the PanAir pressures to the structural grid points. The force vectors are dependent on the size of the structural elements as depicted in Figure 9. A smaller element accumulates pressure from a smaller area. This accounts for the shift in size of force vectors going from inboard to outboard.

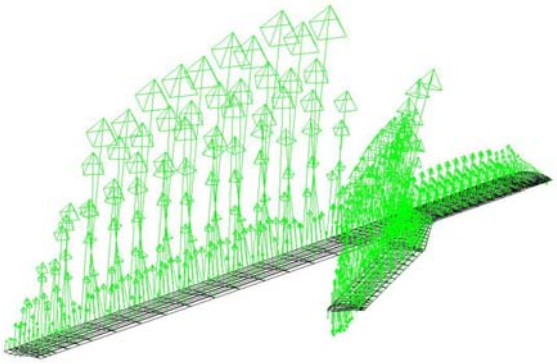

Figure 8. Forces at the structural grid points

Two design models initially were used to arrive at a fully stressed design for the flexible, trimmed loads based on linear finite element analysis. The first model sized element thicknesses according to 16 design variables. The second model independently sized 869 element thicknesses. In the first case, the wing was divided into four partitions: forward wing inboard of the joint, aft wing, joint area, and outboard wing. Within each partition elements were grouped as top skin, bottom skin, spars, and ribs, leading to 16 design variable groups. In both cases, only elements within the confines of the structural wing box (front to rear spars and root to tip ribs) were designed. The design variable linking in the first model turned out to be too coarse. The FSD designed structural mass was ten times greater than the FSD designed structural mass for the second case. Comparison of Figures 9 and 10 demonstrates that the nonlinear response of the aft wing is critical. A linear buckling analysis for the first case indicated that the critical load for stability was exceeded by a factor of three. In a fully geometrically nonlinear analysis, the stress exceeded the linear stress by a factor of 16. These results show the importance of including the geometrically nonlinear response in the design.

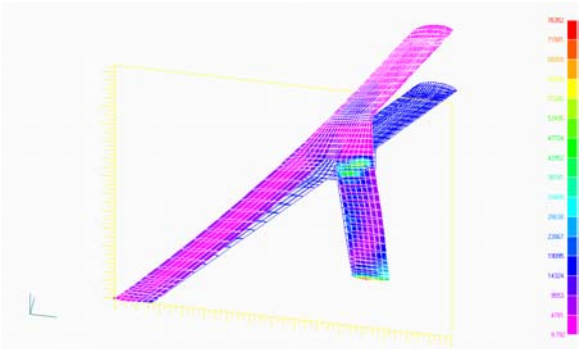

Figure 9. Fully Stressed Design–Linear Analysis

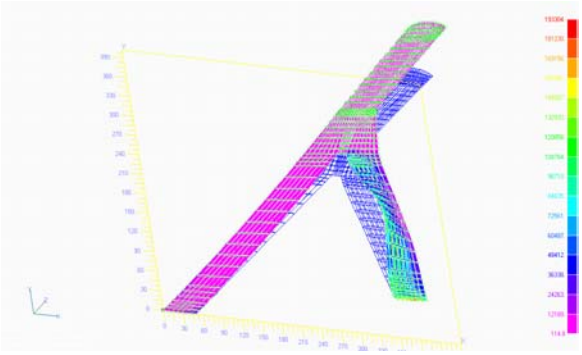

Figure 10. Fully Stressed Design–Non-Linear Analysis

Conclusion

While significant progress has been made, this joined-wing design procedure is not yet complete for developing weight estimations based on non-linear aeroelastic design models. Drag estimation requires a complete model including all effects. Here, induced drag was calculated for wing drag build-up, but a parametric model for parasitic drag was not used. Only a constant parasite drag coefficient of 0.01 was assumed.

After buckling studies using converged PanAir loads, we will turn our attention on converging the combined non-linear aero and structural model to equilibrium condition. This result will be compared with the buckling study to validate the results.

One interesting question needs to be addressed. We have noted that the buckling mode shape tends to unload the outboard wing tip (for washout). We are curious if this effect can be leveraged to produce an aeroelastically fail-safe joined-wing design.

Other aeroelastic issues to be addressed are handling qualities, especially for takeoff and landing in the presence of gusts.

One of the problems that we face is how to optimize a component at the system level. This works if the interactions are relatively minor, such as a conventional structural optimization to minimize weight. For the joined-wing, we need to consider that the antenna may be carrying loads and it certainly will be consuming power and generating heat. Advanced technology suggests that this joined-wing/antenna structure could also be fully adaptive, i.e. actuated to accomplish other functions such as vehicle control and drag reduction. This advanced structure will be completely integrated with the vehicle and the other subsystems, and will need a different approach for credible analysis and optimization.

Acknowledgements

Support from Air Force Office of Scientific Research program manager, Maj. Bill Hilbun, and from Dayton Area Graduate Studies Institute director, Dr. Liz Downie, is gratefully acknowledged.

References

[1] J. Wolkovich., "The Joined-wing: An Overview," Journal of Aircraft, Vol. 23, No. 3, 1986, pp. 161-178.

[2] E. Livne, "Aeroelasticity of Joined-Wing Airplane Configurations: Past Work and Future Challenges – A Survey", AIAA-2001-1370, presented at 42nd AIAA/ASME/ASCE/AHS/ASC Structures, Structural Dynamics and Materials Conference, Seattle, WA, 16-19 April 2001.

[3] M. Blair, T. A. Weisshaar, D. Moorhouse, "System Design Innovation Using MultiDisciplinary Optimization and Simulation", AIAA-2000-4705, presented at the 8th AIAA/USAF/ NASA/ISSMO Symposium on Multidisciplinary Analysis and Optimization at Long Beach CA 6-8 September 2000.

[4] T. A. Weisshaar and D. H. Lee, "Aeroelastic Tailoring of Joined-Wing Configurations", AIAA-2002-1207, presented at 43nd AIAA/ASME/ASCE/AHS/ASC Structures, Structural Dynamics and Materials Conference, Denver, CO, 22-25 April 2002

[5] Sean Wakayama, "Blended-Wing-Body Optimization Problem Setup", AIAA-2000-4740, presented at the 8th AIAA/USAF/NASA/ISSMO Symposium on MultiDisciplinary Analysis and Optimization at Long Beach CA, 6-8 September 2000.

[6] Jamshid A. Samareh, Kumar G. Bhatia, "A Unified Approach to Modeling MultiDisciplinary Interactions", AIAA-2000-4704, presented at the 8th AIAA/USAF/NASA/ISSMO Symposium on Multidisciplinary Analysis and Optimization at Long Beach CA, 6-8 September 2000.

[7] M. Blair and M. H. Love, "Scenario-Based Affordability Assessment Tool", NATO RTO AVT Symposium on Reductions of Military Vehicle Acquisition Time and Cost Through Advanced Modeling and Virtual Product Simulation, Paris France, 22-24 April 2002.

[8] E. Magnus and M. E. Epton, "PAN AIR – A Computer Program for Predicting Subsonic or Supersonic Linear Potential Flows About Arbitrary Configurations Using A Higher Order Panel Method", Vol I – Theory Document, NASA Contractor Report 3251.

[9] Perkins and Hage, Airplane Performance Stability and Control, John Wiley and Sons, Inc., 1949.

[10] S. J. Miley, "A Catalog of Low Reynolds Number Airfoil Data for Wind Turbine Applications", RFP-3387, UC-60, US Department of Energy Wind Energy Technology Division Federal Wind Energy Program, Contract No. DE-AC04-76DP03533.

[11] Lee, Sang H., MSC.Nastran Handbook for Nonlinear Analysis, Volume 1, The MacNeal-Schwendler Corporation, Los Angelos, 1992.

[12] Neill, D. J., E. H. Johnson and R. Canfield (1990). "ASTROS—A Multidisciplinary Automated Structural Design Tool." *Journal of Aircraft*. Vol. 27, No. 12, pp. 1021–1027.

[13] Egbert Torenbeek, Synthesis of Subsonic Airplane Design, Delft University Press, Kluwer Academic Publishers, 1982 (reprinted 1988).

[14] Daniel P. Raymer, Aircraft Design: A Conceptual Approach, AIAA Education Series, 1999.

[15] Leland M. Nicolai, Fundamentals of Aircraft Design, Distributed by METS, Inc., 1975, revised 1984.